

Novel Lamellar Mesostructured Zinc Sulfide Nanofibers

Junping Li, Yao Xu, Dong Wu, and Yuhan Sun*

State Key Laboratory of Coal Conversion, Institute of Coal Chemistry, Chinese Academy of Science, Taiyuan 030001, P. R. China

(Received March 5, 2004; CL-040253)

ZnS nanofibers with lamellar mesostructures were synthesized by hydrothermal reaction of $\text{Zn}(\text{Ac})_2$ and Na_2S using neutral *n*-alkylamines (alkyl = C_8 – C_{16}) as structure-directing template and ethylenediaminetetraacetic acid as stabilizer.

Since the discovery of mesoporous silicates, nanostructured inorganic–organic composites have attracted great interest from the viewpoint of both application and fundamental research.¹ Compared with mesostructured silicates, the construction of non-silicates analogues, especially metal sulfide, presents considerable challenge partly because of the unstable precursor anions and poor understanding of their condensation behavior in solution.² In this respect, there are only a few reports on the synthesis of mesostructured chalcogenides such as CdS ,³ SnS ,⁴ FeS ,⁵ and Ge_4S_{10} .⁶ However, little attention has been paid to the morphology of mesostructured chalcogenides though the specific morphologies may be required for numerous applications in catalysis, chemical sensors, or optical devices.

As typical semiconductor materials of the II–VI group, ZnS nanocrystals have been widely investigated. Various forms of ZnS nanostructures have been synthesized, including nanoparticles,⁷ nanowires,⁸ and nanotubes.⁹ Recently, Yu et al.¹⁰ reported the synthesis of $\text{ZnS}\cdot(\text{NH}_2\text{CH}_2\text{CH}_2\text{NH}_2)_{0.5}$ hybrid nanosheets using the solvothermal routes. In addition, Li and co-workers have also reported the synthesis of hexagonal mesoporous ZnS nanoparticles using cetyltrimethylammonium cations as surfactant.¹¹ Here, we report the synthesis of lamellar mesostructured ZnS nanofibers via mild hydrothermal route using $\text{Zn}(\text{Ac})_2$ and Na_2S as the starting materials in the presence of neutral *n*-alkylamines and ethylenediaminetetraacetic acid (EDTA).

In a typical synthesis, 1.095 g of $\text{Zn}(\text{Ac})_2\cdot\text{H}_2\text{O}$ and 1.60 g of EDTA are mixed in 50 mL of distilled water, together with 3.87 g of octylamine (OA) to form a clear liquid. Then 50 mL of 0.1 mol L^{-1} Na_2S was added to the above liquid. After being stirred for 5 min, the mixture was allowed to react in a 200-mL autoclave at 140°C for 16 h. After the reaction finished, the precipitate was washed with hot water and absolute ethanol repeatedly to remove inorganic and organic residues. Finally, the precipitate was dried at 110°C for 12 h in air. The product can be obtained in about 90% yield based on Zn. The obtained products were characterized by using scanning electron microscopy (SEM), transmission electron microscopy (TEM), powder X-ray diffraction (XRD), and UV–vis absorption spectroscopy.

Figure 1a shows a typical SEM image of the as-synthesized products. It clearly shows that the products are exclusively composed of nanofibers with diameters of about 30 nm and lengths up to several micrometers. A large number of nanofibers exhibit curl morphology and are arranged into bundles, which is further confirmed by TEM (Figure 1b). An HRTEM observation (Figure 1c) reveals that the nanofibers are lamellar mesostructure

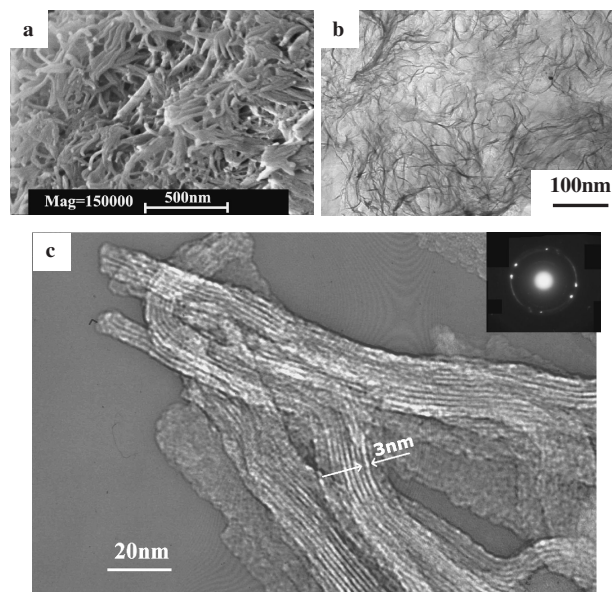


Figure 1. a) SEM, b) TEM, and c) HRTEM images of the ZnS nanofibers; revealing a highly ordered lamellar structure.

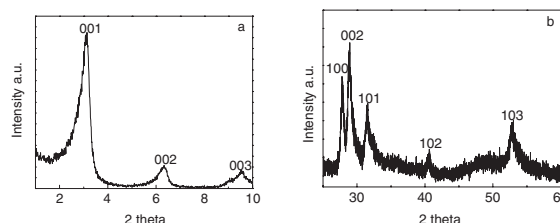


Figure 2. The powder XRD patterns of the ZnS nanofibers: a) low-angle region; b) wide-angle region.

with the layer distance of about 3.0 nm.

The lamellar mesostructure of the samples can be further confirmed by XRD. As shown in Figure 2a, these equidistant diffraction peaks in the low-angle region reveal further the lamellar mesostructure of the products. The *d* spacing of 3.14 nm, corresponding to the first peak in the low-angle XRD pattern, is consistent with the layer distance measured by HRTEM (Figure 1c). The wide-angle XRD patterns of the samples are shown in Figure 2b. In every case, similar peaks are observed, which can be indexed to wurtzite ZnS structure (JCPDS: 36-1450). These diffraction peaks at wide angle generated by the structure within the layers confirm that the layers are composed of crystalline wurtzite ZnS, which is consistent with the corresponding selected area electron diffraction patterns (inset of Figure 1c). When the reaction was carried out in other alkyl-

amines such as decylamine (DA), dodecylamine (DDA), and cetylamine (CTA), a series of lamellar mesostructured ZnS nanofibers were obtained. Interestingly, with the surfactant chain-length increasing, the d spacing increases from 3.1 nm for C₈ to 5.1 nm for C₁₆. Here, the alkylamine acts as template to be intercalated between the ZnS layers so that chain length can alter the spacing of the lamellar structure. However, these reflections in the wide-angle region appear at the same sites independent of the template used.

It was found that EDTA played an important role in the formation of lamellar ZnS nanofibers. Without EDTA, ZnS particles were formed but no lamellar mesostructure was observed. This might be due to the following reason: the direct reaction of Zn²⁺ and S²⁻ is inclined to big ZnS particles that are unable to interact sufficiently with the templates. In the present situation, EDTA as a stabilizing agent binds to the surface of growing ZnS nanocrystals preventing their growth to the bulk phase, and also do not allow the particles to coagulate, which provide desired surface properties for further interaction with the alkylamine templates. Following, the in situ generated ZnS nanoparticles interact with the template and cooperatively assemble into expected hybrid nanostructures before the formation of an insoluble ZnS species.

To further explore the growth mechanism, different hydrothermal durations were investigated. As shown in Figure 3, with the increase of hydrothermal time, the nanofibers became long and thin. However, when the time was decreased to 2 h, the morphology of the products changed from fibrous to sheet-like (Figure 3b). At the same time, it was found that without hydrothermal treatments, the slab-like products (Figure 3a) were formed. This may provide a clue to the growth process of the mesostructured ZnS nanofibers: Under the appropriate hydrothermal conditions, the hybrid nanostructures are exfoliated into thin sheets, and then these exfoliated sheets are curled into nanofibers.

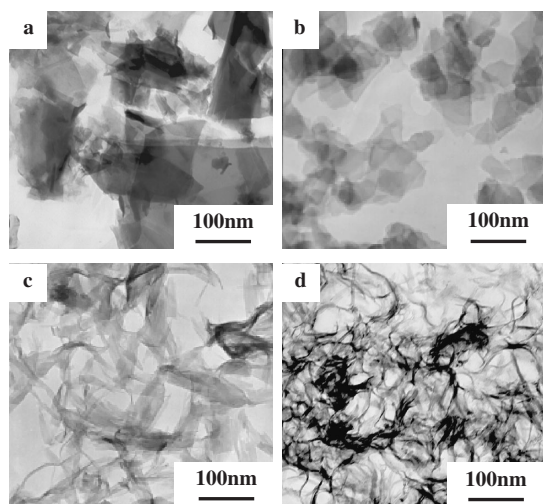


Figure 3. TEM images of the obtained products at 140 °C for different hydrothermal time: a) 0 h, b) 2 h, c) 8 h, and d) 24 h.

It is worth mentioning that the obtained nanofibers exhibit very interesting optical properties. The room temperature UV-vis absorption of the solid powders was shown in Figure 4. Com-

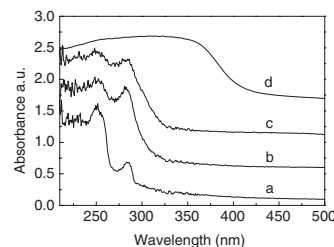


Figure 4. Room-temperature UV-vis absorption spectra of the samples prepared with the different template: (a) C₁₆, (b) C₁₂, (c) C₈, and (d) bulk ZnS powder.

pared with the bulk ZnS (344 nm), the absorption peaks for the nanofibers exhibited a great blue shift. This clearly suggests that the nanofibers have obvious quantum confinement effect.¹² Further work needs to determinate the detailed optical properties.

In summary, ZnS nanofibers with lamellar mesostructures were prepared via a simple hydrothermal route. The UV-vis absorption spectrum shows that the nanofibers exhibit interesting optical properties, and, therefore, are expected that they have potential applications in photocatalysis and optical and electronic devices.

We gratefully acknowledge the support of the National Key Native Science Foundation (Grant No. 20133040).

References

- a) C. Yu, J. Fan, B. Tian, D. Y. Zhao, and G. D. Stucky, *Adv. Mater.*, **14**, 1742 (2002). b) K. Nakajima, D. Lu, J. N. Kondo, I. Tomita, S. Ingaki, M. Hara, S. Hayashi, and K. Domen, *Chem. Lett.*, **32**, 950 (2003). c) M. E. Spahr, P. Bitterli, R. Nesper, M. Müller, F. Krumeich, and H. U. Nissen, *Angew. Chem., Int. Ed.*, **37**, 1263 (1998). d) H. P. Lin and C. P. Tsai, *Chem. Lett.*, **32**, 1092 (2003).
- a) K. K. Rangan, P. N. Trikalitis, C. Canlas, T. Bakas, D. P. Weliky, and M. G. Kanatzidis, *Nano. Lett.*, **2**, 513 (2002). b) F. Schüth, *Chem. Mater.*, **13**, 3184 (2001).
- a) P. Osenar, P. V. Braun, and S. I. Stupp, *Adv. Mater.*, **8**, 1022 (1996). b) P. V. Braun, P. Osenar, and S. I. Stupp, *Nature*, **380**, 325 (1996).
- a) T. Jiang and G. A. Ozin, *J. Mater. Chem.*, **7**, 2213 (1997). b) I. Sokolov, T. Jiang, and G. A. Ozin, *Adv. Mater.*, **10**, 942 (1998).
- J. Li and L. F. Nazar, *Chem. Commun.*, **2000**, 1749.
- a) M. J. MacLachlan, N. Coombs, and G. A. Ozin, *Nature*, **397**, 681 (1999). b) M. J. MacLachlan, N. Coombs, R. L. Bedard, S. White, K. L. Thompson, and G. A. Ozin, *J. Am. Chem. Soc.*, **121**, 12005 (1999).
- E. J. Donahue, A. Roxburgh, and M. Yurchenko, *Mater. Res. Bull.*, **33**, 323 (1998).
- Q. Wu, N. Zheng, Y. Ding, and Y. Li, *Inorg. Chem. Commun.*, **5**, 671 (2002).
- X. Wang, P. Gao, J. Li, C. J. Summers, and Z. L. Wang, *Adv. Mater.*, **14**, 1732 (2002).
- S. H. Yu and M. Yoshimura, *Adv. Mater.*, **14**, 296 (2002).
- J. Li, H. Kessler, M. Soular, L. Khouchaf, and M. H. Tuilier, *Adv. Mater.*, **10**, 946 (1998).
- W. Vogel, P. H. Borse, N. Deshmukh, and S. K. Kulkarni, *Langmuir*, **16**, 2032 (2000).